Multicomponent imaging with distributed acoustic sensing

Ivan Lim Chen Ning & Paul Sava, Center for Wave Phenomena, Colorado School of Mines

SUMMARY

The usage of Distributed Acoustic Sensing (DAS) in geophysics is rapidly gaining popularity due to its dense spatial sampling and low operation cost if the optical fiber is easily accessible. In the borehole environment, optical fibers for DAS are often readily available as a part of other sensing tools, such as for temperature and pressure. Although DAS provides single axial strain measurement along the fiber, the entire strain tensor can also be recovered through a combination of purposefully-designed optical fiber system. Such reconstruction uses multiple strain projections acquired by manipulating the geometry of the optical fiber. The availability of the entire strain tensor opens the possibility for exact elastic wavefield extrapolation, thus avoiding the generation of nonphysical wave modes that contaminate migrated images.

INTRODUCTION

DAS acquires strain along an optical fiber coupled to the ground, which represents the projection of the surrounding strain tensor corresponding to the position of the optical fiber. As shown by Lim and Sava (2017), the reconstruction of the entire strain tensor is possible using multiple strain projections acquired by manipulating the geometry of the optical fiber. They use a configuration with five equally spaced constant pitch angle helical optical fibers and a straight optical fiber to obtain multiple strain projections that sufficiently describe the surrounding strain tensor for the reconstruction. Using six different strain projections, one can reconstruct the entire strain tensor at a given location. This configuration limits the engineering complexity required to build a multi-fiber cable, thus making such data acquisition feasible. Lim and Sava (2017) reconstruct the strain tensor using the information of the strain projections associated with the geometry of the optical fiber, as well as the gauge length captured in an operator defined by the DAS system. This method, therefore, removes the averaging effect in the reconstruction process, which enable the use of the reconstructed strain data as point measurements.

The stress tensor can be obtained from the reconstructed strain tensor if the material properties surrounding the optical fiber are known or estimated accurately. The stress data together with the displacement data can be used for exact elastic wavefield extrapolation, as shown by Ravasi and Curtis (2013). Conventional methods of elastic wavefield extrapolation using only displacement data (i.e. when stress data are not readily available) are heuristic schemes that do not satisfy the reciprocity theorem. Hence, we argue that multicomponent DAS measurements can provide recovery of all information for exact wavefield extrapolation in models of arbitrary complexity. We demonstrate the potential application of multicomponent DAS data with the TTI Marmousi II model adapted from Yan and Sava (2009) and Rocha et al. (2017).

NUMERICAL EXAMPLE

Following the method presented by Lim and Sava (2017), we illustrate the reconstruction of a 3D strain tensor from axial strain measurements along five equally spaced helical optical fibers with constant pitch angle at 20° and a straight optical fiber using synthetic examples of a complex wavefield. The complex wavefields exhibit triplications caused by a velocity model containing a low-velocity Gaussian anomaly, as shown in Figure 1c. We use smaller than usual gauge lengths such as 0.1 m which are possible using specially designed optical fibers, as indicated by Farhadiroushan et al. (2016). The use of a more conventional fiber system with gauge length of 1.0 m is demonstrated by Lim and Sava (2017).

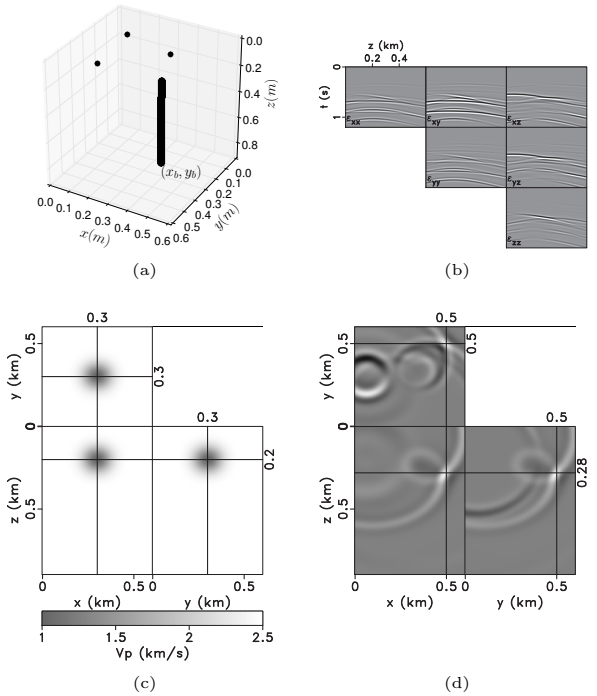

Figure 1: (a) Schematic representation of a DAS experiment depicting the source (dot) and receiver (line) locations. (b) The ideal strain tensor that we would like to reconstruct from DAS measurements. (c) The P-wave velocity model containing a low velocity Gaussian anomaly designed to produce wavefield triplications. The S-wave velocity is half of the P-wave velocity. (d) A snapshot of the vertical displacement wavefield.

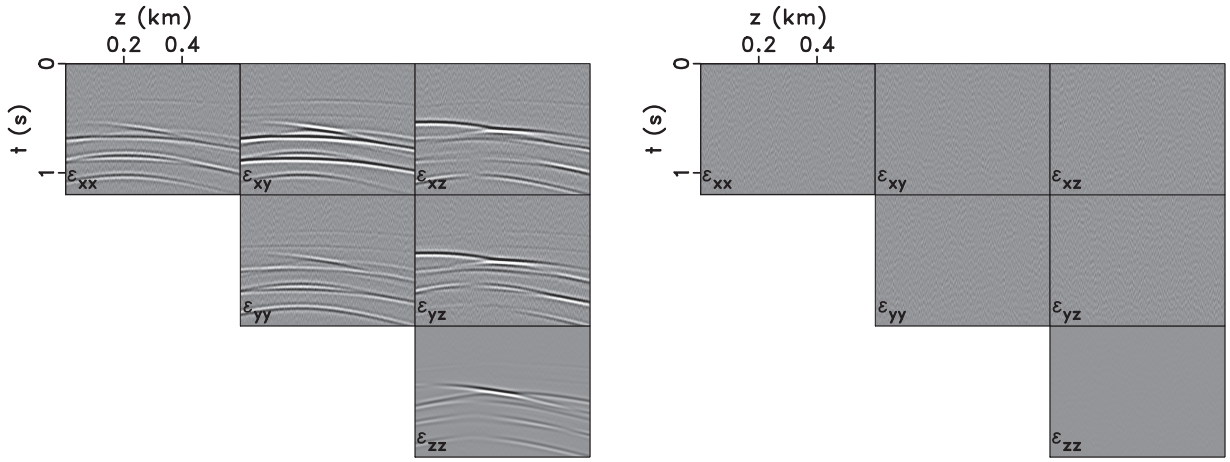

Figure 2: Strain tensor reconstructed from data containing random noise with 10% of the maximum data amplitude and band-limited to the data band with five equally spaced helical optical fibers and a straight optical fiber using a gauge length of (a) 0.1 m. Panel (b) is the difference between the ideal strain tensor in Figure 1b and the reconstructed tensor in (a).

Our numerical setup mimics a simultaneous source experiment with three sources indicated by the dots and the receivers indicated by a straight line of coordinates (x_b, y_b) is shown in Figure 1a. Figure 1b, shown in tensor layout, represents our target strain reconstruction observed along the receiver location at (x_b, y_b). The horizontal and vertical axes of the individual panels represent the distance along optical fiber and time, respectively. We perform the reconstruction by adding random noise with 10% of the maximum amplitude of the data and in the data frequency band. Using a gauge length of 0.1 m, we can reconstruct the strain tensor as shown in Figure 2a. The difference plot in Figure 2b shows no signal leakage and only contain primarily random noise.

In the example using the TTI Marmousi II model (Yan and Sava, 2009; Rocha et al., 2017), we assume that we have access to dense ocean-bottom recordings. We assume the deployment of a multicomponent DAS system, which gives access to both stress and displacement. We adopt the energy imaging condition by Rocha et al. (2017) to produce a single elastic image without wavemode decomposition. Figure 3a shows the single shot image obtained through heuristic wavefield extrapolation using displacement data only. The nonphysical waves present themselves as events crosscutting the geological reflectors, especially in the shallow section. The crosscutting is further highlighted in the zoomed section in the shallow region as illustrated in Figure 3c. However, Figure 3b shows an improved single shot image obtained using exact wavefield extrapolation and the corresponding zoomed section in Figure 3h. The same observation holds for the image obtained after stacking multiple shots. Although the crosscutting in Figure 3a appears to be less severe after stacking in Figure 3e, the geological reflectors are not as coherent when compared to Figure 3f. The effect between heuristic and exact wavefield extrapolation is better illustrated by the zoom sections in the shallow region of the stacked image in Figure 3g and Figure 3h respectively. Extrapolating with both stress and displacement eliminates the nonphysical waves, thus reducing the uncertainty associated with the crosscutting artefacts in our final image.

CONCLUSION

Multicomponent DAS allows us to reconstruct wavefields without the presence of nonphysical waves in the elastic medium. The more accurate wavefields lead to higher quality image, which supports reservoir characterization in complex geological structures. The technique discussed in this paper is applicable to elastic models characterized by arbitrary anisotropy and heterogeneity.

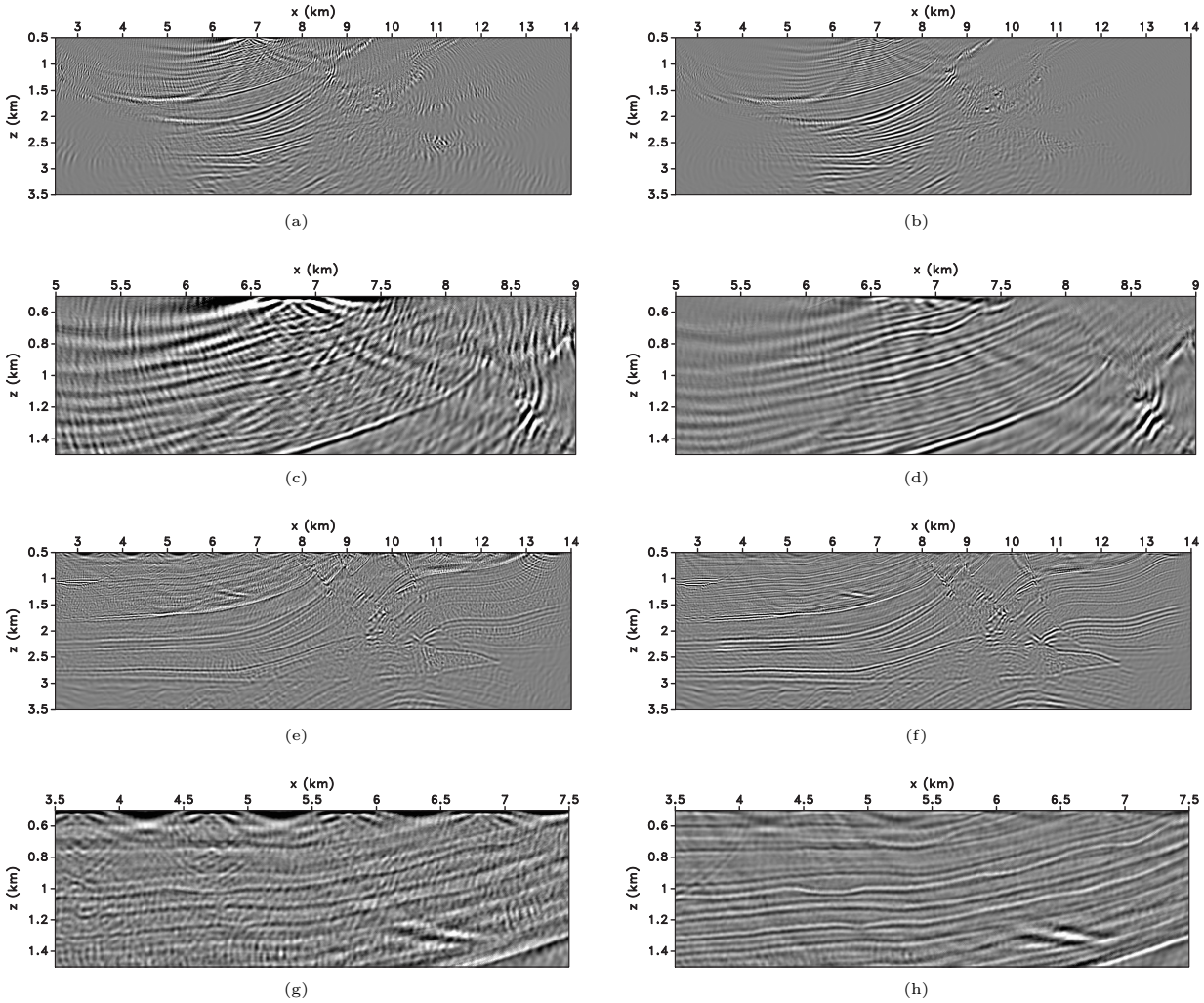

Figure 3: Images obtained using the energy imaging condition from the Marmousi II experiment: (a) **single shot** image using the exact and (b) heuristic wavefield extrapolation. The energy image in panel (c) and (d) is the zoom section of the respective panels in (a) and (b). The **stacked** images in panel use (e) the exact and (f) heuristic wavefield extrapolation. The respective zoom energy image for panel (e) and (f) is shown in (g) and (h).

REFERENCES

Farhadiroushan, M., T. Parker, and S. Shatalin, 2016, Method and apparatus for optical sensing. (WO Patent App. PCT/GB2016/050,625).

Lim, I. C. N., and P. Sava, 2017, High-resolution multicomponent distributed acoustic sensing, *in* SEG Technical Program Expanded Abstracts 2017: Society of Exploration Geophysicists.

Ravasi, M., and A. Curtis, 2013, Elastic imaging with exact wavefield extrapolation for application to ocean-bottom 4C seismic data: Geophysics, **78**, S265–S284.

Rocha, D., N. Tanushev, and P. Sava, 2017, Anisotropic elastic wavefield imaging using the energy norm: Geophysics, **82**, no. 3, S225–S234.

Yan, J., and P. Sava, 2009, Elastic wave-mode separation for vti media: Geophysics, **74**, WB19–WB32.